Confocal Laser Scanning Microscopy and Three-Dimensional Reconstruction of Cell Clusters in Serous Fluids

Claire W. Michael, M.D.,[1]* Judy A.C. King, M.D., Ph.D.,[2] and Raymond B. Hester, Ph.D.[3]

Thick cell clusters are a common finding in reactive and malignant effusions. In order to arrive at a diagnosis, clusters are evaluated for certain cytomorphologic features including size, shape, smooth vs. scalloped borders, and three-dimensional (3-D) configuration. By conventional microscopy, the image of these clusters is often blurred due to limitations in resolution. Consequently, the exact internal structure and cellular arrangement within these clusters cannot be adequately determined.

Utilizing confocal laser scanning microscopy (CLSM), we examined serous fluids from a variety of conditions. Cases included mesothelioma, adenocarcinoma, and papillary adenocarcinoma. Smears were stained with 0.01% ethidium bromide and 1% eosin Y, followed by analysis with an ACAS 570™ image analyzer (Meridian Instruments, Inc. Okemos, MI). Serial confocal fluorescence images were acquired, which allowed 3-D reconstruction of the clusters. Mesothelioma clusters (excluding those with obvious central collagen cores by light microscopy) appeared to be formed of the following configurations: 1) randomly coiled cords of cells, 2) small papillae encompassing central cores, and 3) tissue fragments with pseudoacinar formation. In contrast, adenocarcinomas had a more orderly pattern, with tightly cohesive cells and true acinar formation. Diagn. Cytopathol. 1997;17: 272–279.

Key Words: confocal laser scanning microscopy; serous effusions; mesothelioma; adenocarcinoma

In cytopathology we frequently receive cellular effusions that contain tightly cohesive, solid or hollow, three-dimensional (3-D) cell clusters of different sizes and shapes. The differential diagnosis could be reactive vs. malignant mesothelial proliferation, or mesothelioma vs. adenocarcinoma (Fig. 1A,B). In order to arrive at a diagnosis, we examine these clusters for several morphologic features that have been reported as helpful in the differential diagnosis, e.g., scalloped vs. smooth cell border, or cohesiveness vs. dyscohesion of cells within the cluster. Despite the excellent resolution achieved in the lateral axis by the modern microscope, i.e., the ability to distinguish between two adjacent points in the x and y axes, our ability to examine the vertical, i.e., the z axis, within a thick cluster is greatly compromised. This is because not only those cells in the plane of focus, but also those above and below it, are simultaneously illuminated by the light source, resulting in a blurred image. To overcome this problem, the examiner focuses up and down through the cluster. Confocal laser scanning microscopy (CLSM) allows examination of thick clusters, with the additional ability to optically section through the clusters without the need for embedding and sectioning, analogous to computerized axial tomography. The image is constructed voxel by voxel (volume pixels). Serial fluorescent optical sections are taken at a predetermined interval and consequently reconstructed by the computer into a 3-D image. Such 3-D images can be visualized from any orthogonal or oblique angle by rotating the entire volume.

The optical principles of confocal and epifluorescent (conventional) microscopes are illustrated in Figure C-1, and the differences between them are summarized in Table I. For more details the reader is refered to several excellent reviews of the subject.[1–5]

Our study was undertaken with two objectives: first, to acquire thin optical sections of solid cell clusters retrieved

[1]Department of Pathology, University of Michigan, Ann Arbor, Michigan
[2]Department of Pathology, University of South Alabama, Mobile, Alabama
[3]Department of Microbiology, University of South Alabama, Mobile, Alabama
Presented at the 43rd Annual Scientific Meeting of the American Society of Cytopathology, New York, NY, November 1995.
*Correspondence to: Claire W. Michael, M.D., Department of Pathology, University of Michigan, 1500 E. Medical Center Drive, Room 2G332/Box 0054, Ann Arbor, MI 48109-0054.
Received 16 July 1996; Accepted 21 April 1997

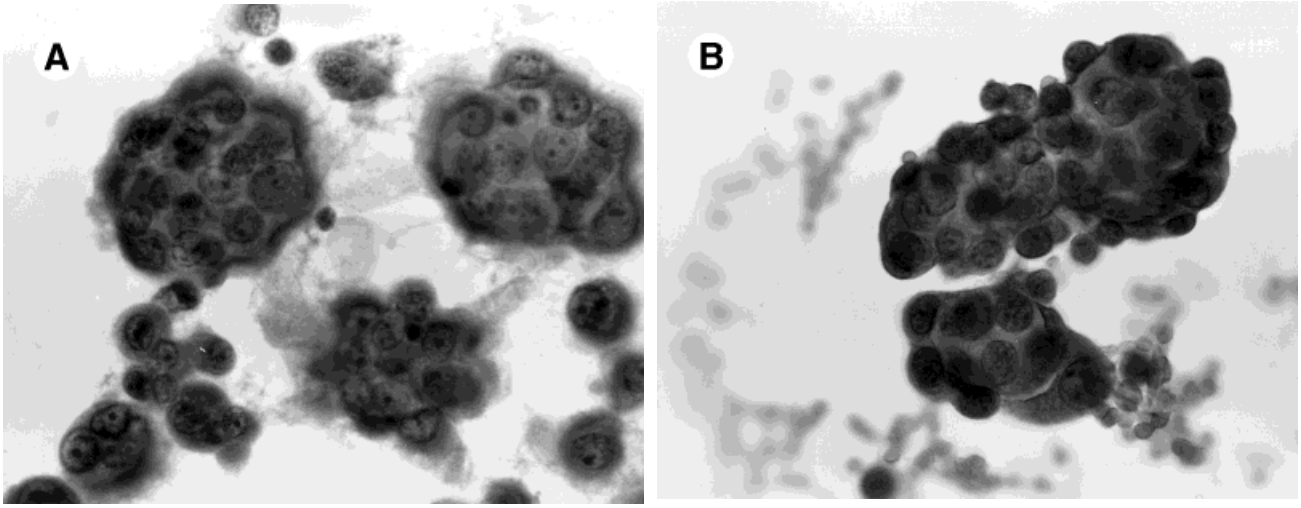

Fig. 1. A: Tight cellular clusters from mesothelioma (Papanicolaou stain, ×400). **B:** Tight cellular clusters from adenocarcinoma. Note similarity to A (Papanicolaou stain, ×400).

Table I.

	Confocal laser scanning microscope	*Conventional epifluorescence microscope*
Illumination source	Laser light, most commonly argon ion laser.	Mercury arc lamp.
Illumination technique	Point scanning: a beam of laser light is focused by a lens on the sample, resulting in illumination of an area of approximately 0.1 µm. The specimen is scanned point by point consecutively. This results in an outstanding axial resolution.	Broadfield imaging: all points in the field of view are illuminated simultaneously (including out-of-focus objects).
Optical pathway	A pinhole with adjustable diameter is incorporated in front of the fluorescence detection system. Fluorescence emitted by objects above and below the focal plane is blocked, and only light emitted from the plane of focus passes through the pinhole. This results in a crisp image with a very good vertical resolution (z-axis).	The image detector system detects fluorescence emitted by the focal plane as well as that above and below it. This results in a relatively blurred image with poor vertical resolution.
Number of colors detected	With CLMS fluorescence, two or more could be detected by the examiner. This is done by incorporating a dichroic filter that splits the light into two photomultiplier tubes that can detect different wavelengths. The computer then overlaps the images detected.	Only one range of wavelength, i.e., color, can be detected at a particular time, depending on the optical filter in the pathway.
Magnification	Through the computer and zoom system, high magnifications approaching those of electron microscopy can be achieved, regardless of the objective magnification.	Limited by the objective magnification.

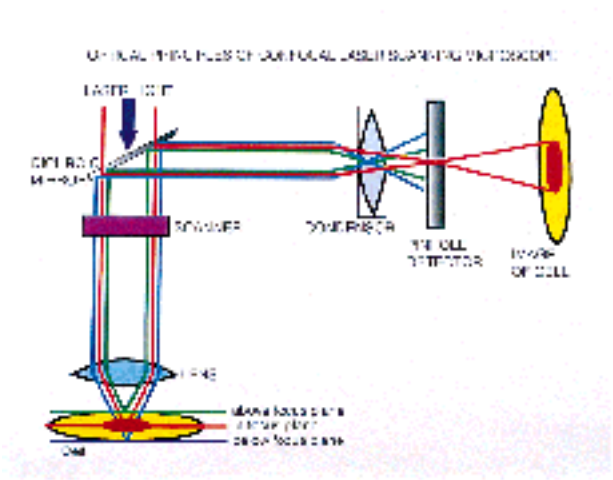

Fig. C-1A

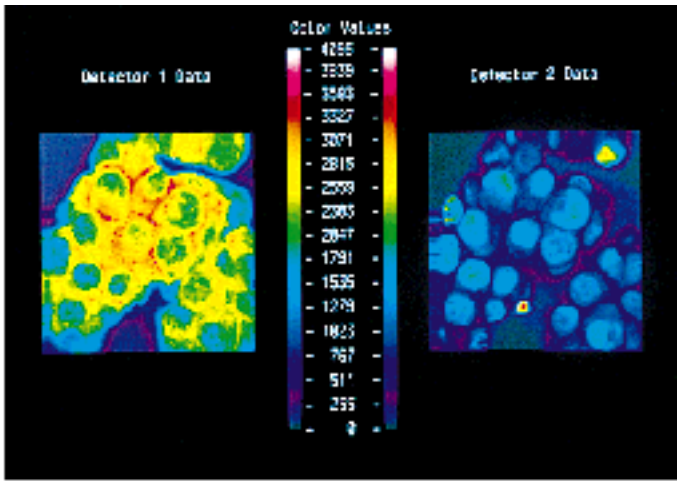

Fig. C-2

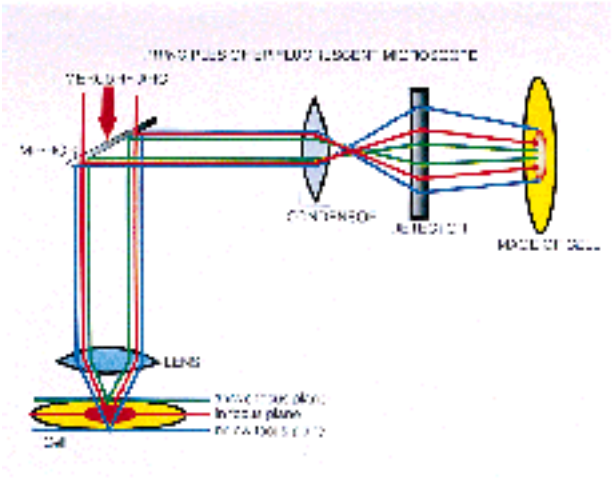

Fig. C-1B

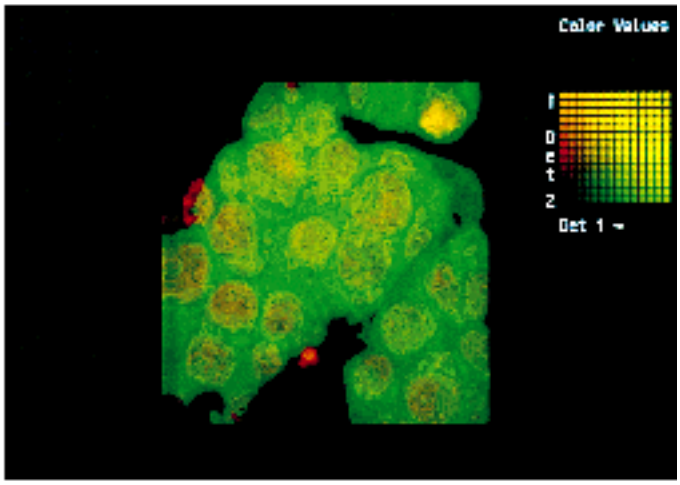

Fig. C-3

Figs. C-1–C-3. Fig. C-1. A: Pathway of light in a confocal microscope. A pinhole is incorporated in front of the image detector. It blocks out-of-focus light and results in a crisp image. **B:** Pathway of light in a conventional epifluorescent microscope. Light reflected from out-of-focus planes results in a relatively blurred image. **Fig. C-2.** Two-color fluorescence. Detector 1 detects eosin fluorescence (cytoplasm), and detector 2 detects ethidium bromide fluorescence (nuclei), as seen in a cluster of mesothelioma. Colors represent a measure of fluorescence intensity. Note increased perinuclear intensity in detector 1. **Fig. C-3.** Images from the two detectors in Figure C-2 are overlapped by the computer to give a two-color fluorescence image. Note wide spacing of cells, with occasional cytoplasmic gaps and ruffled cell surfaces.

from serous fluids with different pathologic conditions followed by reconstruction of 3-D images, and second, to examine the structural configurations and cellular relationships within these clusters in order to identify any features that can differentiate adenocarcinoma from mesothelioma.

Materials and Methods

Aliquots of the effusions were collected in 50-ml disposable plastic tubes and centrifuged at 2,000 rpm for 10 min. The supernatants were decanted. One to two drops of the sediment were pipetted onto a slide and smeared by the two-slide pull technique. At least six slides were prepared for each case, and the remaining material was used for cell block preparations. Two slides were air-dried, and the remaining four were immediately sprayed with Surgipath® cytology fixative (Surgipath Medical Industries, Grayslake, IL). For cytologic evaluation, one air-dried smear was stained by the Diff-Quik method (Baxter Healthcare, Miami, FL), and two fixed smears were stained by the Papanicolaou method. The remaining three smears were prepared for evaluation by CLSM.

Our study included cytologic smears from 2 cases of malignant mesothelioma, 4 cases of adenocarcinoma, and 1 case of a borderline papillary serous tumor of extraovarian mesothelium. To distinguish mesothelial vs. epithelial origin, a battery of immunoperoxidase stains, which included high and low molecular weight keratin, carcinoembryonic antigen, epithelial membrane antigen, and B72.3, was per-

formed on cell blocks from the two mesotheliomas and two adenocarcinomas. Histologic sections of the primary tumors were also reviewed in all 7 cases.

The staining procedure for confocal microscopy was adopted from Boon et al. and King et al., as previously described:[6–8]

1. Rehydrate (from 100% ethanol to 60% ethanol).
2. Rinse in tap water and deionized water.
3. Stain with 1% eosin Y (in deionized water) for 1 min (pH 7.0) (Fisher Scientific, Pittsburgh, PA).
4. Rinse in deionized water.
5. Stain with 0.01% ethidium bromide (EtdBr) for 3 min (pH 5.7) (Curtin Matheson Scientific, Inc., Houston, TX).
6. Rinse in deionized water.
7. Mount the coverslip (#1) with Aqua-Mount® (Lerner Laboratories, Pittsburgh, PA).

Some smears were stained only with EtdBr to selectively stain the nuclei.

Selection of Clusters

The stained slides were reviewed with an Olympus BX 50 fluorescence microscope (Olympus America, Lake Success, NY). Thick cell clusters were selected and dotted by a permanent marker. Confocal microscopy was performed by a nonpathologist who was not informed of the nature of the examined clusters at the time of acquiring the images. The images were subsequently evaluated by two pathologists who were aware of the diagnoses.

CLSM

The smears were examined with an ACAS 570™ image analyzer (Meridian Instruments, Okemos, MI). The ACAS 570 is equipped with an Innova® 90-5 5-watt argon ion laser (Coherent®, Palo Alto, CA) and an Olympus IMT-2 inverted microscope. Emitted fluorescence was collected through an Olympus Dapo 100 UV (NA = 1.3 oil) objective.

The 488-nm laser line was used to excite both EtdBr and eosin Y. The optical filter setup included a 530/30 band pass filter for detection of eosin fluorescence in front of photomultiplier tube 1 (PMT 1), a 605 long-pass filter in front of PMT 2 (detection of EtdBr), and a 575 short-pass dichroic filter to split the emitted fluorescence between the two PMTs (Fig. C-2). The images collected in both detectors are then overlaid to produce a two-color fluorescence image (Fig. C-3).

PMT sensitivity, laser power, and laser scan strength varied, with typical settings being 35% PMT sensitivity, 100 mW laser power, 10% scan strength, and a 1% neutral density filter. Settings were adjusted for optimal visualization, without photobleaching of sample fluorescence, using the ACAS 570 Optimize program. Magnification and resolution of the pseudocolor image were determined by the number of sample points taken in the x and y axes, the distance between sample points, and the number of samples collected and averaged at each point.

Confocal Imaging of Clusters

Confocal images were collected at either 0.3- or 0.5-µm z-intervals with a pinhole setting of 80 µm. An average of 5–10 clusters was examined from each case. Depending on the thickness of the cluster, between 50–100 optical sections of 640 × 480 pixels each were collected and stored on 20MB Bernoulli cartridges (Iomega Corp., Roy, UT). The 3-D reconstruction was performed using Meridian Simulated Fluorescence Process software (SFP). The SFP combines a series of thin optical sections into one 3-D image, and then projects it against a reflective background.

Results

Our results are summarized in Table II.

Adenocarcinoma

Adenocarcinoma clusters ranged between 20–40 µm in thickness. Examination of serial sections (Fig. 2A) revealed one or more true acini (hollow structures or lumens surrounded by a continuous cell layer at the same plane and having continuity with the consecutive planes; cells lining the top and bottom of these lumens could be traced). The cells forming these acinar structures were closely packed and showed luminal orientation (Fig. 2B). Their nuclei were crowded, oval, and molded. The chromatin distribution was much coarser and the nuclear membranes were more irregular than those of mesothelioma. Prominent nucleoli were frequently seen, and occasionally macronucleoli were detected. On 3-D reconstruction, the cells within the cluster were tightly cohesive and related to each other in an organized fashion, with the formation of true lumens (Fig. 2C). The cells forming the circumference of the cluster had a common cell border, with the long axis of their nuclei aligned parallel to the circumference and resulting in a smooth appearance.

Results of the case of borderline serous tumor of the mesothelium with psammoma bodies were separately reported.[8] In summary, we demonstrated that the psammoma bodies, rather than being a complete sphere, were in fact cylindrical structures surrounded by epithelial cells with the exception of one side. Also, on occasion the clusters seemed to result from branching of the original body. These findings were supportive of the theory that psammoma bodies form in the stalks of vascular papillae. The tips of the papillae may break off, leaving an epithelial bare edge.[9,10]

Mesothelioma

Mesothelioma clusters were similar in thickness to those of adenocarcinoma. Only solid aggregates with no obvious

Table II. Differences Between Mesothelioma and Adenocarcinoma by CLSM

Feature	*Mesothelioma*	*Adenocarcinoma*
Cell-to-cell relationship	Relatively spaced, with window formation	Tightly cohesive and crowded
Cytoplasm		
Surface	Ruffled	Smooth
Quantity	Relatively abundant	Variable
Staining	Higher perinuclear intensity	No differential staining
Nucleus		
Contour	Irregular	Irregular
Chromatin	Coarse, with occasional clumping	Clumping and abnormal distribution more obvious
Nucleoli	Small	Visible, more prominent
Internal structure		
Acinar formation	Pseudoacini	True acini
Orientation of cells	Haphazard	Luminal
Orientation at the circumference	Perpendicular, resulting in a scalloped appearance	Parallel, resulting in a smooth appearance
Variety of structure		
Tissue fragments	Present	Present
Papillae	Always seen	Only in papillary adenocarcinoma
Coiled sheets of cells	Frequently seen	Rarely present

central collagen cores by light microscopy were selected for CLSM. The abnormal chromatin distribution and irregular nuclear contours were easily appreciated on thin sections. Occasionally, nucleoli were easily discernible; however, they were not commonly seen. The cytoplasm showed a differential staining pattern, with higher intensity at the perinuclear area and lower intensity towards the periphery (Fig. C-2). The cells were spaced apart and had ruffled cytoplasmic borders, and windows between adjacent cells could be seen when closely examined (Fig. C-3). In some cases, the nuclei were crowded and aggregated, perhaps representing multinucleated mesothelial cells (Fig. 3). Examination of serial sections revealed several patterns of cellular arrangement. Some clusters were paucicellular in the center, with the cells mainly located at the periphery surrounding an apparent space, suggestive of a central core (Fig. 4). Other clusters appeared to be formed by a cord of cells which resembled a thread of beads that coiled around itself in a random manner (Fig. 5). Pseudoacinar formation was frequent, in which a possible lumen appeared in one section but continuity was lost in the consecutive levels (Fig. 6A). Multiple pseudoacini could be detected within the same cluster. The cells forming these pseudoacini, however, did not show luminal orientation, but appeared to randomly surround these central spaces.

On 3-D reconstruction the cells within the clusters were loosely associated and stacked in different planes (Fig. 6B). No true lumens were identified. The cells forming the circumference of the clusters resembled cotton balls, with the long axis of their nuclei aligned perpendicular to the surface, which resulted in a scalloped appearance.

Technical Issues

Cytologic smears were optimal for this study, since the clusters were all intact and did not have the truncation effect seen in paraffin-embedded thick sections. However, the clusters were slightly flattened by the smear preparation technique. This required smaller intervals (0.3 μm) between the consecutive optical sections, and consequently a longer duration in imaging individual clusters. Images from fixed smears were superior to those that were air-dried. Air-drying resulted in further flattening of the clusters and increased background staining. Uncoated or electrically charged slides were easier to examine than coated slides. The latter had higher background staining, which interfered with calibrating the intensity of the two-color fluorescence utilized in our study. Also, the stains had to be freshly prepared with an optimal pH. Utilizing stains that were neither fresh nor at an appropriate pH resulted in an altered fluorescence intensity and leaking of the EtdBr into the cytoplasm (Fig. 7). Photobleaching could be avoided by storing stained slides in the dark at 4°C for up to a few weeks. It was noted, however, that after a few days the intensity of eosin Y autofluorescence declined much faster than that of EtdBr.

Discussion

Serous effusions occur in a variety of pathologic conditions. Cytologic examination of these fluids is usually the first step taken in the patients' workup, since it is cost-effective and relatively less invasive, and carries a much lower risk of tumor dissemination compared to open biopsy.

The differential diagnosis between malignant mesothelioma and adenocarcinoma remains a challenging problem

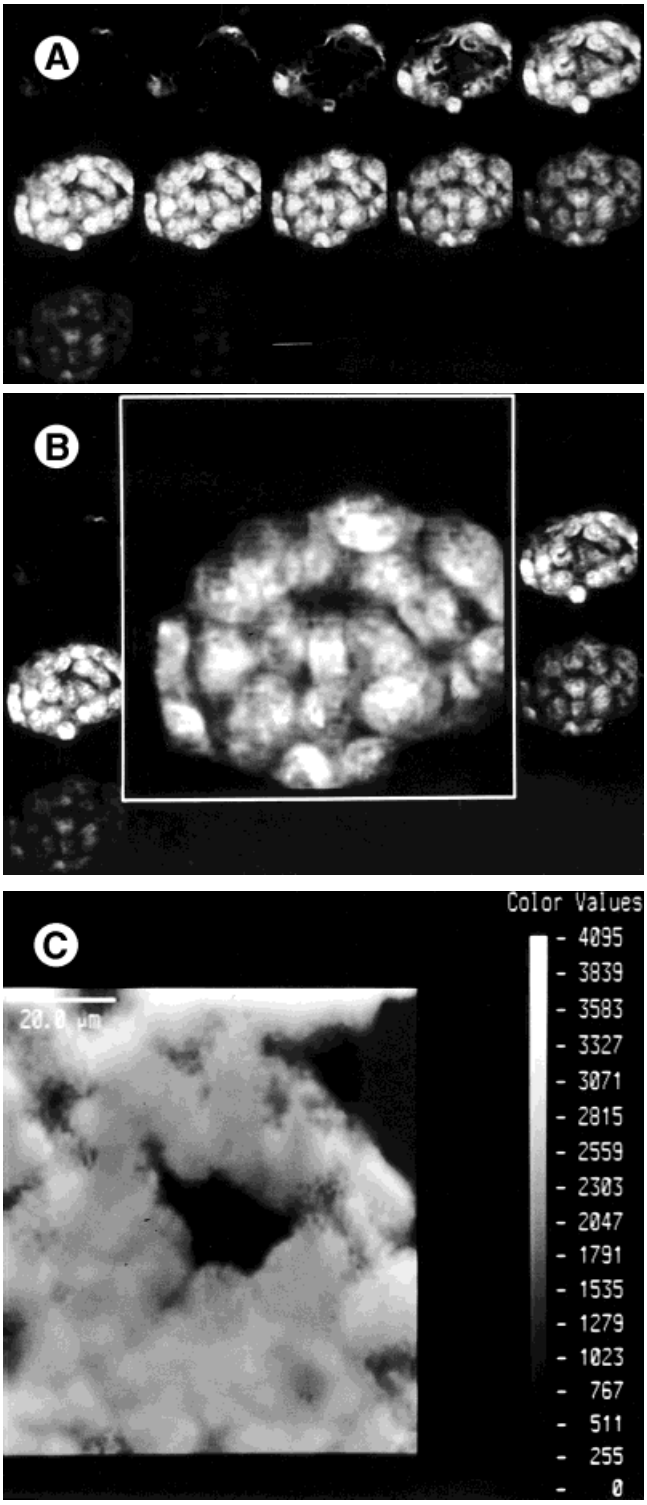

Fig. 2. A: CLSM serial optical sections of an adenocarcinoma cluster. Note true lumen formation (ethidium bromide and eosin Y stain). **B:** Magnified optical section emphasizing true acinar formation, with closely packed cells showing luminal orientation (ethidium bromide and eosin Y stain). **C:** Three-dimensional reconstruction. Magnified image demonstrates true acinus within a cluster of adenocarcinoma (ethidium bromide and eosin Y stain).

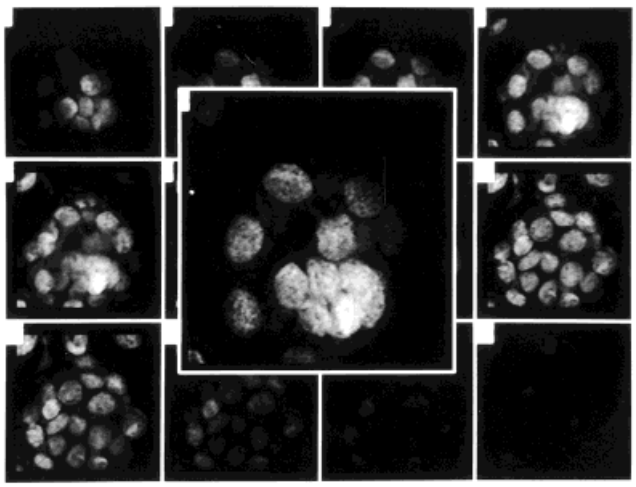

Fig. 3. Optical sections of a mesothelioma cluster, showing local aggregation of the nuclei (ethedium bromide).

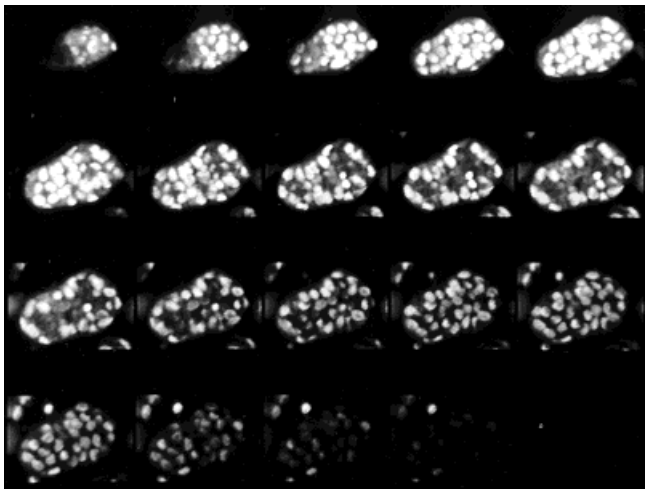

Fig. 4. Serial optical sections of a mesothelioma cluster. Note the paucicellularity of the center in the sections of the second and third rows (ethidium bromide).

to pathologists. Because spherical and papillary cell aggregates are an essential diagnostic feature of mesothelioma, they have been the subject of study by several researchers, who described their morphology and labeled them with a variety of names,[11–13] e.g., rounded cell conglomerates, morules, spheres, papillae, and adenomatous structures. However, similar cell aggregates also occurred in adenocarcinoma and certain reactive effusions, rendering diagnosis of some cases difficult. These numerous names and descriptions reflected the diversity of morphology of these aggregates, whose internal structure remained a mystery to the pathologist. How were these clusters formed in vivo? Were they broken-off papillae? Were they formed by simple exfoliation of the tumor? Or did the cells roll around each

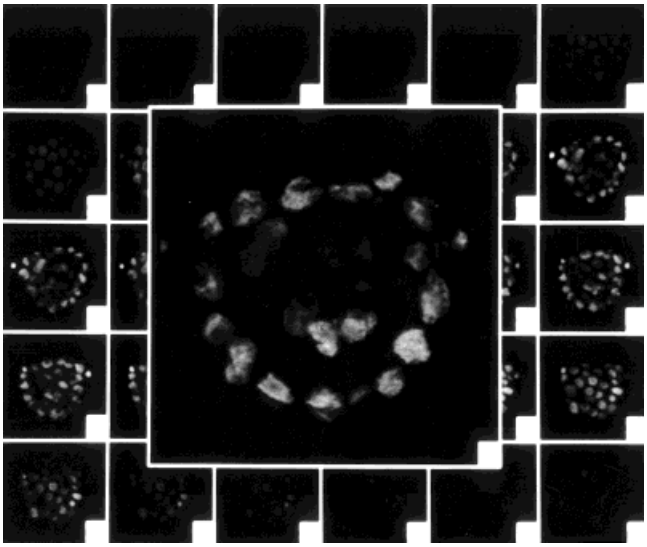

Fig. 5. Serial optical sections of a mesothelioma cluster. Note coiling of cells within the space to form a sphere (ethidium bromide).

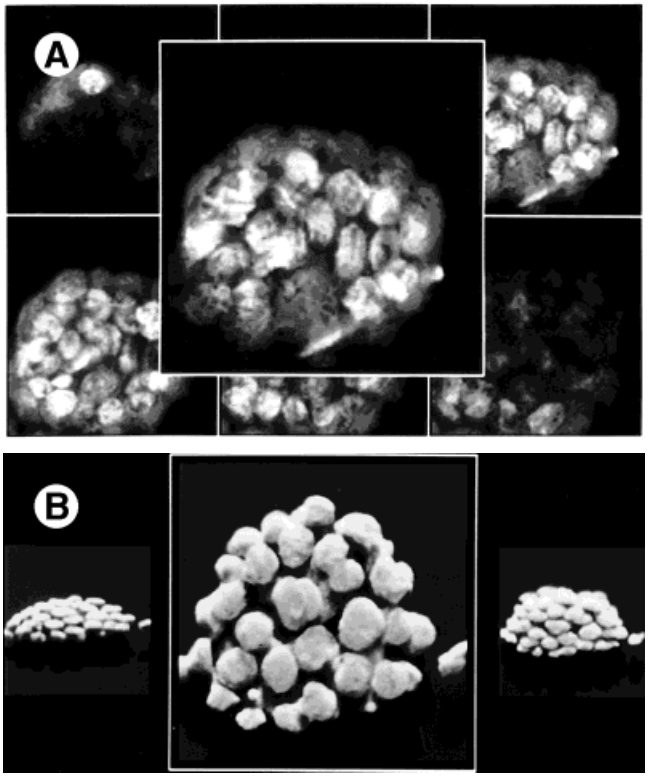

Fig. 6. A: Thin optical sections of a mesothelioma cluster. Note pseudoacinar formation, in which luminal orientation of the cells and continuity with the consecutive levels are lacking (ethedium bromide and eosin Y stain). **B:** Three-dimensional reconstruction of a mesothelioma cluster, rotated in different angles. Note lack of lumens, loose association of cells, and scalloped border (ethedium bromide).

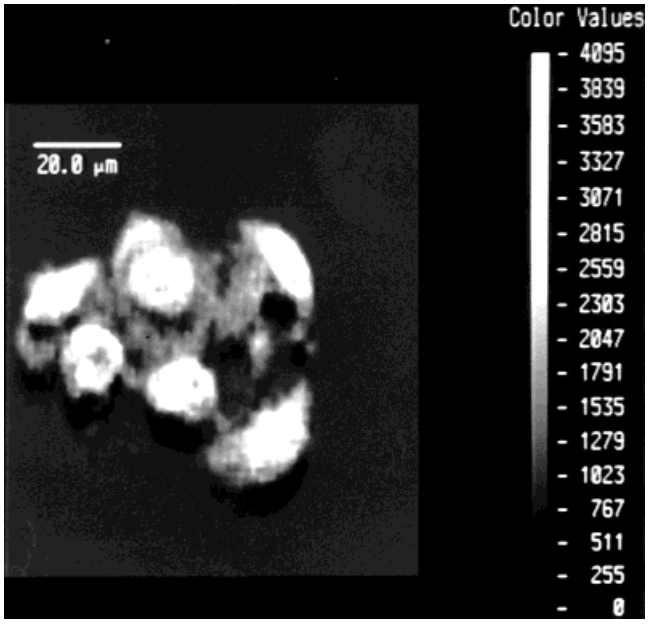

Fig. 7. Example of a 3-D reconstructed image of an adenocarcinoma cluster stained with an inappropriate pH. Note leaking of stain into the cytoplasm (ethedium bromide).

other in the fluid? Because of the limitations in vertical resolution of the conventional microscope, the examiner has to focus up and down throughout the thickness of the cluster in order to evaluate its internal structure. The resulting image is still suboptimal and blurred, since the planes above and below the plane of focus are simultaneously excited by the light source. Hence the questions remained unanswered.

In the late 1970s, Whitaker[14] noticed that in one mesothelioma case, some aggregates contained a central, amorphous, eosinophilic material. This material did not stain with periodic acid-Schiff (PAS), and stained bright blue with Martius scarlet blue (MBS), suggesting that it could be collagen. The Van Gieson stain further confirmed these findings. By electron microscopy, the aggregates were formed of a ring of cells surrounding a central core. Higher resolution of that central core demonstrated fibrillar whorls with a periodicity of 640 Å, further confirming its collagenous nature. These results prompted study of an additional 11 cases of mesothelioma and 80 pleural and peritoneal effusions with various metastatic carcinomas. It was found that 4 of the 12 (33%) mesotheliomas had similar findings, but only 2 of the 80 (2.54%) carcinomas had collagen within their aggregates. Based on these findings it was suggested that these aggregates represented broken-off papillae.

In the past, construction of a 3-D image of similar spherical structures would involve examination of numerous, stained, semiserial 5-µm-thick sections of the paraffin-embedded tissue. Successive drawings of the morphology in each section would be prepared using a profile projector. Graphic reconstruction of a 3-D image would be made by

presenting the successive drawings in a stereogram, and the connections between different structures would be demonstrated in a linear diagram.[15] This procedure is tedious and time-consuming, and requires a great deal of imagination. With CLSM, this can be achieved more efficiently and accurately by the computer-assisted 3-D reconstruction of serial thin optical sections, eliminating the need for embedding, sectioning, drawing, and tracing. The resolution of the computer image is excellent, and the 3-D reconstruction can be manipulated and rotated in different angles according to the needs of the investigator. In this study, we examined tightly cohesive cell clusters from serous effusions with a variety of pathologic conditions, to explore their internal structure and further contribute to the literature with our findings.

Our preliminary results indicate that there are certain differences in the internal structure of clusters between those of mesothelial vs. epithelial origin. While cases of adenocarcinoma persistently showed an organized structure with true acinar formation, mesotheliomas showed an array of structures. True acinar formation with luminal orientation of the cells was consistently lacking in mesotheliomas, which displayed a rather pseudoacinar pattern. Moreover, the cells in mesotheliomas were haphazardly arranged and had wider intercellular spaces in comparison to those of adenocarcinomas. On high-power magnification, cell windows and ruffled cytoplasmic surfaces could be appreciated in mesotheliomas. Some clusters appeared like a thread of beads coiled around itself to form a sphere. Other clusters revealed an empty central core, probably corresponding to the collagen cores described by Whitaker.[14] These findings suggest that while adenocarcinoma clusters may be formed by exfoliation of parts of the parent tumor with preservation of the microacinar formation, the mesothelial clusters are probably formed by several processes. In addition to tumor exfoliation, some of these mesothelial clusters represent broken-off papillae, while others are sheets of cells that form spheres once emersed in the fluid.

In conclusion, in this preliminary report we have presented differences in the internal structure of the tight cell clusters of adenocarcinoma and mesothelioma. We have also demonstrated the diversity of structure of mesothelioma clusters, reflecting the various descriptions they acquired in the past. Studies on a larger series of cases would be useful to assess the diagnostic utility of this technique.

References

1. Shotten DM. Confocal scanning optical microscopy and its applications for biological specimens. J Cell Sci 1989;94:175–206.
2. Sasano H, Date F, Itakura Y, Goukon Y, Nishihira T, Nagura H. Confocal laser scanning microscopy in cytopathology. Mod Pathol 1993;6:625–629.
3. Tekola P, Zhu Q, Baak JPA. Confocal laser microscopy and image processing for three-dimensional microscopy: technical principles and an application to breast cancer. Hum Pathol 1994;25:12–21.
4. Rigaut JP, Vassy J, Herlin P, et al. Three-dimensional DNA image cytometry by confocal scanning laser microscopy in thick tissue blocks. Cytometry 1991;12:511–524.
5. Matsumoto B, Kramer T. Theory and applications of confocal microscopy. Cell Vision 1994;1:190–198.
6. Boon ME, Schut JJ, Suurmeijer AJH, Benita EM, Hut PKH, Kok LP. Confocal microscopy of false-negative breast aspirates. Diagn Cytopathol 1995;12:42–50.
7. Boon ME, Kok LP, Sutedja G, Dutrieux RP. Confocal sectioning of thick, otherwise undiagnosable cell groupings in cervical smears. Acta Cytol 1993;37:40–48.
8. King JAC, Hester RB, Titford ME, Michael C. Psammoma bodies: confocal microscopy with 3-D reconstruction of two-color fluorescence on paraffin-embedded sections and cytology smears. Cell Vision 1995;2:420–424.
9. Ferenczy A, Talens M, Zoghby M, Husain SS. Ultrastructural studies on the morphogenesis of psammoma bodies in ovarian serous neoplasia. Cancer 1977;39:2451–2459.
10. Johannessen JV, Sobrinho-Simões M. The origin and significance of thyroid psammoma bodies. Lab Invest 1980;3:287–296.
11. Bonito L, Giovanni F, Colautti I, Bonafacio D, Dudine S, Giarelli L. Cytopathology of malignant mesothelioma: a study of its patterns and histological bases. Diagn Cytopathol 1993;9:25–31.
12. Triol JH, Conston AS, Chandler SV. Malignant mesothelioma: cytopathology of 75 cases seen in a New Jersey community hospital. Acta Cytol 1984;28:37–45.
13. Berge T, Gröntoft O. Cytologic diagnosis of malignant pleural mesothelioma. Acta Cytol 1965;9:207–212.
14. Whitaker D. Cell aggregates in malignant mesothelioma. Acta Cytol 1977;21:236–239.
15. Ohuchi N, Rikiya A, Kasai M. Possible cancerous change of intraductal papillomas of the breast. Cancer 1984;54:605–611.